A. Baars and A. Delgado

Start-up behaviour of a natural circulation evaporator in brewing industry

The start-up behaviour of a wort kettle with a steam heated internal reboiler has been investigated using an open, single tube (length 2.3 m, inner diameter 44.3 mm), steam heated natural circulation evaporator. Hereby, the influence of heating steam pressures (0.18 to 0.45 MPa), hydrostatic head *H* with water for process medium has been evaluated. This work implies the description of appearing operational modes during start-up, the time for the start-up process and the development of parameter constellations for a gentle heating up of the process medium. On the course to a stationary behaviour with saturated boiling at the outlet of the evaporator, different transient and stationary operational modes can arise e.g. geysering coupled with manometer oscillations followed by a stationary mode, density wave oscillations type I, and a stationary mode with subcooled boiling. Geysering and density wave oscillations feature a strong periodic behaviour. The former mode may lead to serious degradation of wort and apparatus. The transition of modes can be accompanied by a more or less short-time random behaviour of the circulating mass flow. The course of operational states strongly depends on the parameter settings and the flow pattern in the kettle. Geysering disappears with increasing heating steam pressure and decreasing hydrostatic head. The heating up process is accelerated by rising heating steam pressure and hydrostatic head. In contrast, a more gentle mechanical and thermal treatment of the process medium was obtained with decreasing values for *H*.

Descriptors: start-up, natural circulation, evaporator, operational behaviour, oscillation, wort kettle, internal reboiler

1 Introduction

For quality of beer, the bio-chemical reactions during wort boiling prove to be of high importance, e.g. precipitation and coagulation of proteins, removal of unwanted volatiles, extraction and isomerisation of hop components, sterilization of wort and colour build up [1, 2]. In case of biomaterials, the history of processing has to be taken into consideration. Both, excessive and insufficient thermal processing exerts a negative effect on the quality of the final product. Different wort boiling systems are in the market. Mezger, Krottenthaler and Back give an overview in [3]. A widely used reactor for wort boiling in industry is the wort kettle with internal reboiler with volumes of up to 120 m^3. This system consists of a cylindrical tank and contains a centrally positioned tube bundle heat exchanger. On the shell side, the exchanger is optionally heated by steam or by pressurized water. On the tube side, wort is partially evaporated. The two phase mixture leaves the heat exchanger, is accelerated in the succeeding nozzle and reaches the bulk liquid by deflection plates. In case of the subjet system, the deflection plates are located under the wort level [4, 5]. Due to change in density in evaporator and nozzle, natural circulation sets in. For a defined treatment of wort, flow pattern in the kettle, the operational behaviour of the reboiler as well as their interactions proves to be crucial. In the field of flow pattern in wort kettles with internal reboiler a variety of works has been carried out by [6, 7, 8, 9, 10, 11]. In the domain of natural circulation evaporators in general, a variety of contributions is available in literature. This results from the simple construction of the apparatus without moving elements. From this, several advantages arise such as low expenditure of investment, running costs and maintenance. Therefore, this type of evaporator is widely used in industry: conventional / nuclear power plants [12, 13], chemical-, environmental-, food engineering, biotechnology [14, 15, 16]. In comparison to evaporators with pumps, the discussed system characterises a mechanically gentle processing of the process medium, especially interesting for liquid biomaterials such as wort [17]. On the other hand, the operational behaviour of natural circulation evaporators proves to be strong nonlinear [18, 19] and the mass flow of feeding liquid can only be set indirectly. Chen et al. [20] relate the former phenomenon to "the delicate balance between gravity head available due to downcomer and various pressure losses in the loop".

In praxis, a stable two-phase flow [21] and fully developed boiling at the outlet of the heat exchanger/evaporator is preferred. For a given geometry, this operational state only arises at certain constellations of process parameters. Alternatively, a variety of stationary and transient modes can appear. A comprehensive and systematic overview to transient operational behaviour in evaporators give Bouré et al. [22] and Yadigaroglu [23].

During start-up, the subcooling of the process medium decreases. Hence, the state of the system changes with time. On the way to the final mode, different operational behaviours can emerge [18]. This is especially the case if no external pressurizing of the system is performed. A typical course of start-up modes at low system pressures consists of (a) a stable single-phase flow at high subcooling followed by (b) geysering/flashing and/or (c) density wave oscillations type I, (d) a stable two-phase flow at low subcooling, see [18, 21, 24 – 28]. Investigations to geysering/flashing have been carried out for the first time by Griffith [29]. In the following different types of geysering have been recognized by [19, 26, 27, 30, 31]. Yadigaroglu [23] gives a detailed description of density wave oscillations (DWO). Fukuda and Kobori [32] recognized two different types of this mode: type I with nearly zero steam quality and type II with relatively high steam quality at the exit of the evaporator.

Albert Baars, Dr.-Ing. Albert Baars, Institute of Fluid Mechanics (LSTM-Erlangen), Friedrich-Alexander-University Erlangen-Nuremberg, Cauerstr. 4, D-91058 Erlangen, baars@mytum.de; Prof. Dr.-Ing. Antonio Delgado, Institute of Fluid Mechanics (LSTM-Erlangen), Friedrich-Alexander-University Erlangen-Nuremberg, Cauerstr. 4, D-91058 Erlangen.

Tables and figures see Appendix

Up to now, a couple of procedures has been investigated to prevent or minimize oscillations in natural circulation evaporators during start-up. In various publications [21, 28, 33, 34], the increase in pressure drop in the feeding line is recognized to reduce the intensity of oscillations and to shift the region of instability to higher inlet subcooling and lower heat fluxes. Lee and Pan [33] explain this effect with the reduced gravitational pressure drop contribution relative to the frictional contribution which stabilizes the system. A further possibility to minimize oscillating modes consists of the increase in system pressure. Here, a stationary mode can be reached at higher inlet subcooling and lower heat fluxes. Corresponding investigations have been carried out by [25, 26, 35]. Jiang et al. [36] applied nitrogen to pressurize the system.

In this contribution, the start-up behaviour of a single, steam heated natural circulation evaporator is investigated for heating steam pressures of 0.18 to 0.45 MPa, different hydrostatic heads, water for process medium, and an evaporator tube of industrial size. Experiments have been carried out under dynamic conditions: due to heat input, the temperature of the process medium continually rises with time until the final operational state is obtained. The continuous decrease of subcouling of the process medium distinguishes this contribution from own previously published works [19, 34, 37] and enables the analysis of time required for start-up. Furthermore, this work implies the description of the appearing operational modes. In addition, parameter constellations are presented with focus on a gentle heating up of the process medium. This is especially of interest for the sensitive liquid biomaterial wort.

2 Material and Methods

2.1 Apparatus

The test facility consists of a u-tube connected to a feeding tank (1) and a steam separator (4) at its open ends (see Fig. 1). The two tanks are linked to each other by a horizontal tube. One side of the u-tube is steam heated (3). The pressure drop coefficient of the feeding line to the evaporator (3) can be set by a ball valve (2). The steam heated tube in the evaporator with a heated length of 2.3 m, an inner diameter of 44.3 mm and a wall thickness of 2 mm features an electro polished inner wall. The pressure drop coefficient in the feeding line without throttling amounts to $\zeta_1 = 0.4$. The heating steam pressure is controlled. Before entering the shell side of the evaporator, a steam dryer separates the liquid from the vapour phase of the heating steam. After condensation, the liquid leaves the evaporator by a ball float trap and a condensate cooler to avoid evaporation as a result of pressure release.

All tanks, the evaporator and its feeding line possess inspection windows for observation of two phase flow pattern and the shape of liquid surfaces, respectively. The tubes and tanks consist of stainless steel. Insulation of the apparatus with glass fibre minimises heat losses.

The hydrostatic head H represents the vertical distance between outlet of the two-phase mixture at the deflection plate and the liquid wort surface in the kettle. In case of $H \leq 0$, the subjet configuration exists, see e.g. [4, 5]. A full transfer of findings obtained from this experimental set-up to praxis cannot be guaranteed, even if the heated tube and the thermal boundary conditions are of industrial scale. This results mainly from the partial geometrical similarity of the experimental set-up with respect to an industrial wort kettle. Nevertheless, valuable information about the influence of relevant parameters on the operational behaviour and possible solutions can be obtained.

2.2 Data acquisition

Platinum thermometers (PT 100) in 4-wire technique in casing pipes (diameter 2 mm, wall thickness 0.2 mm) serve for temperature measurements at inlet, outlet of the evaporator, and in the feeding tank (TIR in Fig. 1). The sensors have been calibrated together with the transmitters. The volume flux in the u-tube (FIR) is determined by a magnetic inductive flowmeter (Endress and Hauser, Promag 33 H). A pressure transmitter by Haenni (ED 510) detects the pressure of heating steam (PIRC). A PLC (programmable logic controller) by Texas Instruments (Type 545) controls the heating steam pressure. For data acquisition, a board by National Instruments (PCI-MIO-16E-4) and LabView is used in combination with a personal computer.

2.3 Experimental procedure /Data analysis

The initial temperature of each start-up experiment amounts to 30 °C (subcooling ≈ 70 °C). The volume of process medium is set as follows: under flow conditions (a) the liquid level in the steam separator is localized at the lower edge of the connecting pipe and (b) the liquid level in the feeding tank with the distance H below it. After, the heating steam pressure p is adjusted. All experiments have been carried out with water as working fluid. Ambient pressure exists in the head spaces of feeding tank and steam separator. The parameters and the investigated ranges are listed in Table 1. With opening of the steam valve, the data are recorded every 0.1 s until a stationary mode with saturated condition at the outlet of the heat exchanger is obtained.

3 Results

In the following, all results are presented in dimensionless form. In Table 2 the relevant quantities are listed.

The time t and the time period T are normalized with the time period T_U of the isothermal liquid flow manometer oscillations of the investigated system, see below and in [20]. In case of the dimensionless mass flow $\dot{m}^*$ identical densities of the origin and referred mass flow are supposed. The velocity at the inlet of the evaporator v_l is divided by the characteristic velocity L_H / T_U to obtain $\dot{m}^*$, where L_H denotes the length of the heated tube. The subcooling $\Delta\vartheta_{X\ Sub}$ is defined as difference between boiling (B) and the relevant temperature ϑ_X. The quantities ρ_l and ρ_g represent the density of liquid and the vapour phase, c_p the thermal capacity as well as r the enthalpy of evaporation.

At the chosen parameter constellation, all observed operational modes within these investigations appear. The sequence starts with geysering at higher subcooling, followed by an intermediate state I, steady state I, intermediate state II, density wave oscillations type I (DWO), steady state II at subcooled, and then at saturated condition. The progression of modes resembles descriptions in literature by Schuster et al. [18]. With decreasing subcooling, they find a stable single-phase flow followed by geysering, hydrostatic head fluctuations, density wave oscillations type I, and stable two phase flow. During start-up, the appearance of operational modes strongly depends on the parameter settings. This will be shown after an introduction of the individual modes.

3.1 Geysering coupled with manometer oscillations

This operational state shows the most violent behaviour of all observed modes within this investigation. The periodic ejection of fluid out of the evaporator leads to remarkable vibrations of the experimental set-up. Figure 3 depicts the mass flow in the heat

exchanger, and the subcooling at inlet / outlet of the heat exchanger versus time. This mode follows the typical sequence of geysering described by Yadigaroglu [23]: (a) vapour generation/expulsion, (b) refilling, and (c) incubation.

The first phase (a) starts with a sudden generation of bigger amounts of vapour which leads to an ejection of vapour/liquid mixture to both sides of the heat exchanger. This can be recognized by the shape of the mass flow curve, marked by the arrow in Figure 3, and by visual observations. In the following, the two phase flow is accelerated towards the steam separator by buoyancy force. Due to the change of geodetic height and acceleration of the liquid phase, flashing occurs. The mass flow reaches the maximum and the subcoolings at the inlet a minimum. Then, subcooled liquid from the feeding tank enters the heated tube. Due to the insufficient residence time of the liquid in the heat exchanger, vapour generation and in the following the mass flow decrease. The sequence continues with the refilling (b) of the heated zone. Hereby, liquid displaces the gas phase completely. With the onset of backflow, incubation (c) begins. The liquid in the heated zone is partially heated up to a saturated/superheated state (see negative values of $N_{I\,Sub}$ in Fig. 3) and the sequence restarts by vapour generation.

This mode characterises an interaction between pure geysering and manometer oscillations. Experiments under isothermal conditions reveal weakly damped manometer oscillations with a periodic time

$$T_U = 2\pi\sqrt{L/g}$$

and

$$L = \sum_i \frac{A_S}{A} L_i \quad .$$

Hereby, g, L_i and A_i describe the gravitational acceleration, the lengths and the cross sectional areas of all liquid filled tubes/tanks of the u-tube and A_S the cross sectional area of the feeding tank. The comparison of this analytical solution with experimental data delivers a maximum deviation of 3.6 %.

The existence of manometer oscillations can be observed during refilling and incubation. In the first phase, a partial change from kinetic to potential energy occurs. After onset of incubation, conversion from potential energy to kinetic energy takes place. With vapour generation, this process stops and kinetic energy is fed to the process medium. Due to the latter phenomenon the manometer oscillations are maintained. The mass flow curve in Figure 3 exhibits no complete period of manometer oscillation – the periodic time of the isothermal manometer oscillations is greater than that of the geyser. In Figure 4(a) the periodic time T^* is plotted versus τ in dimensionless form. The values of T^* are inferior to one and decrease under-proportionally with time. This results from the decreasing subcooling of the feeding liquid and leads to shorter incubation periods of the oscillation. For more detailed analysis of this operational state, see [19].

3.2 DWO

Density wave oscillations are often described in literature (e.g. [22, 23, 34]). Therefore, the mechanism is not explained in detail, here. Figure 5 plots the mass flow, subcooling at inlet (I) and exit (E) versus time in dimensionless form. The mass flow is characterised by the typical nearly sinusoidal behaviour. The periodic time and the amplitude exhibit lower values in comparison to geysering and decreases with τ (Fig. 4(b)) due to the declining subcooling of the feeding liquid. During appearance of DWO, the mean value of the mass flow rises notedly due to increased vapour generation. The latter phenomenon occurs temporarily and leads then to higher gravitational pressure drop. On the other hand the frictional pressure drop does not rise adequately. Hence, the mass flow rises and the residence time decreases. In the following, the vapour generation cannot be maintained and the mass flow diminishes. The fluctuations of mass flow induce enthalpy fluctuations in the single phase part of the heat exchanger. After the liquid has passed the boiling boundary, these are converted to fluctuations of void fraction and gravitational pressure drop. This acts back to the liquid phase and induces again enthalpy fluctuations. The weak negative values of the subcooling number $N_{E\,Sub}$ indicate a superheated state of the fluid at the exit of the evaporator. This results from the hydrostatic pressure of the liquid water column above in the steam separator.

The rising mass flow indicates that this operational mode is governed by buoyancy forces. Fukuda and Kobori [32] denote this as DWO type I. The subcooling at the inlet of the heat exchanger features partially a periodic trend due to backflow of the fluid in the entry. In comparison to geysering, DWO can hardly be detected by temperature oscillations at the chosen locations. This results from the different amplitude of the oscillations. Further information to this operation state delivers also [34].

3.3 Intermediate states, steady state I and II

The intermediate states connect geysering, respectively DWO with steady state I. They show a similar behaviour of the adjoining, transient states but are less periodic. In the passage to the steady state, sinusoidal, decaying respectively kindling oscillations arise (Fig. 2). The steady states are characterised by more or less random, small amplitude oscillations of the mass flow, which result from perturbations due to bubble generation and the two phase flow in the heated channel. In the case of steady state I, the decreasing subcooling of the feeding liquid leads to a slight increase in mass flow with time. Steady state II and therefore saturated boiling emerge asymptotically, illustrated by the temporal course of mass flow, feeding and inlet subcooling in Fig. 2.

3.4 Interaction evaporator – periphery

The temporal appearance of the different operational states strongly depends on the flow in steam separator, feeding tank and feeding line. The flow pattern determines the temperature course at the inlet of the heated tube, which represents an essential boundary condition. On the other side, a remarkable influence of the operational behaviour of the evaporator on the transport processes in the connected apparatuses exists. This leads to complex interactions with feedback effects. In the following, the analysis of the measured subcoolings and the mass flow in the experimental set-up delivers a certain understanding of these interactions, without focussing on detailed flow investigations.

It can be assumed, that the steam separator features most homogeneous temperature distribution in comparison to the other apparatuses because (a) it is the smallest vessel and (b) during operation, the fluid (vapour and liquid) enters the vessel mostly from the bottom in form of a free jet.

A closer look to the subcooling of feeding and inlet liquid in Fig. 2 reveals for geysering during vapour generation and expulsion temporarily nearly equal temperatures ($\tau = 18...32$). This indicates a certain mixing effect in feeding tank and feeding line due to flow oscillations. This concerns especially the feeding tank during backflow, where a free jet enters the vessel from the bottom. Like geysering, steady state I characterises low effective conveyed mass, therefore low time averaged flow velocities in feeding tank and line. In contrast to geysering, negligible flow oscillations appear in

the set-up, which lead to development of a temperature stratification in feeding tank and feeding line. After onset of steady state I ($\tau \approx 36$ in Fig. 2), subcooling at the inlet remains constant for a certain time, while the subcooling in the feeding tank decreases. This supports the hypothesis of well mixed flow in the apparatuses during geysering. At $\tau \approx 48$ the temperature stratification has reached the inlet of the heated tube, the subcooling at the inlet of the evaporator starts to decrease. Between the beginning of steady state I and this point of time, equal inlet subcooling exists. Hence, (a) during this period the mass flow remains constant due to constant inlet conditions of the evaporator and (b) the slopes of the subcooling in the feeding tank at $\tau \approx 36$ and at the inlet at $\tau \approx 48$ show nearly same values. Small deviations in case of (b) result from diffusive and convective energy transport in flow direction. For $\tau > 48$, decreasing inlet subcoolings lead to rising flow velocities. Hence, (a) for $\tau > 36$, $\tau > 48$, respectively, the slopes of subcoolings differ and (b) the subcooling at the inlet $N_{I\ Sub}$ goes asymptotically to $N_{F\ Sub}$. At onset of intermediate state II, these two subcooling numbers show nearly the same values. These effects have to be expected also in an industrial wort kettle. Their dominance depends amongst others strongly on the flow pattern in the kettle, as shown here.

3.5 Stability Maps

As stated before, the operational behaviour of the investigated system depends on the parameter settings and the state of the process medium. Further on, the latter quantities are represented by the subcooling number in the feeding tank $N_{F\,Sub}$. Fig. 6 displays a plane of $N_{F\,Sub}$ and Jacob number N_{Ja} for different liquid charging levels H with

$$N_{Ja} = \frac{c_p(\vartheta_{HS} - \vartheta_B)}{r} \frac{\rho_l - \rho_g}{\rho_g} \quad , \qquad (1)$$

where the intermediate states are not explicitly plotted. The value $N_{F\,Sub}$ represents a function of time during start-up and v_{HS} denotes the heating steam temperature. In literature, often a plane of subcooling number $N_{F\,Sub}$ and phase change number N_{pch} respectively Zuber number N_{Zu} or a subcooling $\Delta\vartheta_{Sub}$ versus heat flow $\dot{Q}$ plane are used for stability maps [24, 25]. In this case, the choice of N_{Ja} instead of N_{Zu} results from the different thermal boundary condition. Due to steam heating, a nearly constant temperature at the boundary of the heated tube exists instead of a constant heat flow. Furthermore, the mass flow in the Zuber number is not a parameter but arises in a natural circulation evaporator in dependence of plant geometry and process parameters. To indicate a relation between N_{Ja} and N_{Zu} for the investigated system, Baars [37] has proposed a simple power law model containing a modified Zuber number N_{Zu+}.

$$N_{Zu+} = C_1\, N_{Ja}^{m}\, N_{F\,Sub}^{1-n} \qquad (2)$$

with

$$N_{Zu+} = \frac{\dot{Q}}{A_H \rho_l \sqrt{g\, d\, r}} \frac{\rho_l - \rho_g}{\rho_g}$$

The relation does not consider the different operational states. For the investigated parameter range, the constants result to $C_1 = 0.04319$, $m = 1.1$ and $n = 0{,}75$. The value A_H represents the cross sectional area of the heated tube and d the diameter of the connecting tube (Fig. 1). The relation exhibits an accuracy of ±20 %. It points out the expected result that the heat flow increases with rising heating steam temperature and subcooling of the feeding liquid.

For all settings, density wave oscillations arise on the way from subcooled to saturated boiling. Furthermore, with rising N_{Ja} the transitions of modes appear at higher subcoolings. Similar experimental and theoretical results at low quality conditions have been reported in literature, e.g. [13, 25, 33].

The parameter liquid charging level H has a significant influence on the topology of the stability map. With rising liquid charging level, the change from DWO to steady state II moves to lower subcoolings. Here, H acts partially conversely to N_{Ja} on the transition of modes. At $H = 0$ mm during start-up, the well known succession of modes of natural circulation evaporators arises: steady state at high subcoolings, density wave oscillations type I and steady state at low subcooling/saturated state. At $H \geq 12.5$ mm (no Figure), lower Jacob and higher subcooling numbers, geysering replaces steady state I. A further change of the map topology appears at $H = 100$ mm: steady state I arises between geysering and DWO. The latter phenomenon indicates that there exist parameter constellations, where the hydrostatic head can exert a similar effect on the operational behaviour like the frictional pressure drop. Even if the mechanisms of these pressure drops are different, both act conversely to the gravitational pressure drop.

3.6 Heating-up time

For a gentle mechanical and homogeneous thermal treatment of sensitive biomaterials, not only the type of operational state but also the duration of treatment during start-up proves to be of high importance. Fig. 7 displays the time τ, the different operational states occur during start-up, until steady state II is reached. The data are presented for a start temperature of 68 °C (subcooling ≈ 32 K).

The time τ to reach a specific operational state decreases overproportionally with the Jacob number due to a rise in heat flow. In comparison to N_{Ja}, the hydrostatic head exerts no significant influence on τ concerning the transitions to DWO and steady state II. Also, no tendency is observable.

On the other hand, the transition to steady state II appears at decreasing subcoolings with growing H (Fig. 6). This may result from the higher residence time of the fluid in the evaporator with increased H. Hence, the fluid reaches saturated state at lower inlet subcooling. At this point the question arises, if the hydrostatic head H exerts any influence on the warm-up time (time the system requires to heat up the process medium to a certain temperature). Fig. 8 depicts this time τ versus N_{Ja} for different temperatures (ϑ_F = 75, 85 and 95 °C). The warm-up time decrease with N_{Ja}, H and decelerate with growing ϑ_F. The first and the last effect can be explained by the impact of N_{Ja} and ϑ_F on the heat flow, see Eq. (2). The influence of the liquid charging level H on τ may be attributed to the effect that with rising H, transient operational modes appear preferably, whereby convective heat transfer is enhanced.

To estimate the warm-up time without considering the effects of the different operational states, Eq. (2) can be applied. Due to the appearance of subcooled boiling during start-up, this relation considers both, the heat flow for evaporation and for heating up the liquid phase. To account only for the heat flow which contributes to the heating up of the liquid, a function $f(H)$ is introduced, which was received by adaptation to the own experimental data

$$N_{Zu+,\,l} = f(H)\; C_1\; N_{Ja}^{m} N_{Sub}^{1-n} \tag{3}$$

with

$$f(H) = C_2\; \exp(C_3\, H / d).$$

According to the latter relation with the constants C_2 = 0.5 und C_3 = 0.01677, approximately half to two third of the transferred heat flow in the investigated parameter range contributes to heat up the liquid phase. The remaining part leads to evaporation of the process medium. Furthermore, this result shows, that convective heat transfer is enhanced with rising H. This may come from the augmented occurrence of transient operational states. The dimensionless warm-up time τ is received by inserting Eq. (3) into

$$\dot{Q} = mc_p \frac{d\vartheta_F}{dt}$$

and in the following by integration

$$\tau = \frac{t}{t_c} = \frac{N_{F\,Sub0}^{n} - N_{F\,Sub}^{n}}{n C_1\, f(H)\; N_{Ja}^{m}} \tag{4}$$

with

$$t_c = \frac{m}{A_H \sqrt{g\, d}\; \rho_l}\ .$$

The variable t_c represents a characteristic time, $N_{F\,Sub0}$ the initial subcooling number of the process medium, and m the mass of the process medium in the system. The latter value is assumed to be constant during start-up. The relation is valid for subcooling numbers greater than zero, hence superheating is not taken into account. Eq. (4) implies the simplifying assumption of a local independent temperature of the liquid in the system – or of ideal mixing in the periphery, respectively. Despite the simplifications, a quite good agreement between experimental and predicted data appears for $N_{Ja} > 100$ (see Fig. 8). The later observations may be explained by increased mass flow und therefore enhanced mixing in the tanks and the feeding line with growing N_{Ja}.

4 Summary

Experiments with a one tube, steam heated natural circulation evaporator (heating steam pressures 0.18 to 0.45 MPa) have been carried out with water as process medium at ambient pressure to investigate the start-up behaviour of a wort kettle with internal reboiler. The heated tube of 2.3 m length and 44.3 mm inner diameter features industrial size. Depending on the parameter constellation and with decreasing subcooling of the process medium, the results reveal a succession of different transient and stationary modes. Hereby, the parameters hydrostatic head H (represents the vertical distance between outlet of the wort at the reflection plates and the wort surface), heating steam pressure and the flow pattern in the process medium in the kettle outside of the internal reboiler proves to be of significant influence. At H = 0 mm (subjet configuration), first stationary state with subcooled boiling appears followed by density wave oscillations type I (DWO) before the target mode stationary state with saturated boiling sets in. With increasing H (> 12.5 mm), a further operational state arises – geysering. At H = 100 mm the succession geysering, stationary state with subcooled boiling, DWO and stationary state with saturated boiling appears. Geysering proves to be the most violent operational state which may lead to a strong and heterogeneous thermal as well as mechanical treatment of wort and apparatus. Low hydrostatic heads and higher heating steam pressure can avoid this operational mode, whereby the former alternative leads towards a more gentle heating-up process of wort. In contrast to heating steam pressure, the parameter H exerts only a weak influence on heating-up time. For estimation of the latter quantity, a simple algorithm is delivered.

5 Bibliography

1. Narziß, L.: Die Technologie der Würzebereitung. 7. Auflage, Ferdinand Enke Verlag, Stuttgart, 1992.
2. Narziß, L.; Back, W.: Abriß der Brauerei. 6. Auflage. Wiley – VCH, Weinheim, 2005.
3. Mezger, R.; Krottenthaler, M.; Back, W.: Modern Wort Boiling Systems – an Overview, Brauwelt International **21** (2003), Nr. 1, pp. 34-39.
4. Baars, A.; Herbster, T.; Schmidt, T.; Delgado, A.: Realisierung einer technologiegerechten Durchströmung der Würzepfanne mit Innenkocher durch gezielte Modifikation der Geometrie, Brauwelt **144** (2004), pp. 1164-1166.
5. Biwanski, T.; Baars, A.; Delgado, A.; Schmidt, T.; Bühler, T.: The subjet wort boiling system of low expenditure and high benefit, Proc. 30th EBC Congress (2005), p. P81, Fachverlag Hans Carl, Nürnberg, Germany.
6. Baars, A; Walk, U; Werner, F; Delgado, A: Untersuchung der Strömung in einer Würzepfanne mit Innenkocher, Der Weihenstephaner **68** (2000), pp. 16-19.
7. Baars, A.; Werner, F.; Delgado, A.: Numerische Untersuchung der Strömung in einer Würzepfanne während der thermischen Würzebehandlung, LVT, **45** (2000), pp. 203-206.
8. Baars, A.; Herbster, T.; Delgado, A.: Laseroptische Messungen in einem technischen Behälter mit Naturumlaufverdampfer, Proc. 11. Fachtagung „Lasermethoden in der Strömungsmesstechnik“ GALA (2003), Braunschweig, pp. 27.1-27.6.
9. Delgado, A.; Baars, A.; Herbster, T.: Improvement of wort treatment in a kettle with an internal natural boiler, Proc. 29th EBC Congr. (2003), pp. 25/1-25/11, Fachverlag Hans Carl, Nürnberg, Germany.
10. Biwanski, T.; Baars, A.; Kowalczyk, W.; Delgado, A.: Investigation of the flow in an industrial reactor with internal evaporator, Proc. Int. Symp. Research-Education-Technology (2005), Gdansk, Poland, pp. 35-42.
11. Biwanski, T.; Baars, A.; Kowalczyk, W.; Delgado, A.: Flow structure in a technical scale reactor with an internal reboiler, PAMM, 6 (2006), pp. 467-468.
12. Hibi, K.; Ono, H.; Kanagawa T.: Integrated modular water reactor (IMR) design, Nuclear Engineering and Design, **230** (2004), pp. 153-266.
13. Nayak, A.K.; Vijayan, P.K.; Saha, D.; Venkat Raj, V.; Aritomi, M.: Study on the stability behaviour of a natural circulation pressure tube type boiling water reactor, Nuclear Engineering and Design, **215** (2002), pp. 127-137.
14. Hills, J.H.; Jones, W.E.; Ibrahim, A.K.: The behaviour of a pilot-scale horizontal thermosyphon reboiler, Trans. IChemE, **75** (1997), pp. A 652-656.
15. Sloley, A.W.: Properly design thermosyphon reboilers, Chem. Eng. Progr., 3 (1997), pp. 52-64.
16. Baars, A.; Werner, F.; Delgado, A.: Investigations on the maximum inner wall temperature in a steam heated tube with natural circulation for the use in biotechnology, in: B.J. Grochal, J. Mikielewicz,

B. Sunden (Eds.), Proc. 3rd Baltic Heat Transfer Conf. (1999), pp. 509-514, IFFM Publishers, Gdansk, Poland.

17. Brück, D.: Einfluss mechanischer Belastungen auf dispergierte, empfindliche Inhaltsstoffe von Flüssigkeiten in Leitungssystemen und Behälterströmungen, Dissertation, Technische Universität München, 1997.
18. Schuster, C.; Ellinger, A.; Knorr, J.: Analysis of flow instabilities at the natural circulation loop DANTON with regard to non-linear effects, Heat and Mass Transfer **36** (2000), pp. 557-565.
19. Baars, A.; Delgado, A.: Nonlinear effects in a natural circulation evaporator: Geysering coupled with manometer oscillations, Heat and Mass Transfer, **43** (2007), pp. 427-438. (DOI 10.1007/s00231-005-0069-3)
20. Chen, W.L.; Wang, S.B.; Twu, S.S.; Chung, C.R.; Pan, C.: Hysteresis effect in a double channel natural circulation loop, International Journal of Multiphase Flow **27** (2001), pp 171-187.
21. Kim, J.M.; Lee, S.Y.: Experimental observation of flow instability in a semi-closed two-phase natural circulation loop, Nuclear Engineering and Design **196** (2000), pp. 359–367.
22. Bouré, J.A.; Bergles, A.E.; Tong, L.S.: Review of two-phase flow instability, Nuclear Engineering and Design **25** (1973), pp. 165-192.
23. Yadigaroglu, G.: Two-phase flow instabilities and propagation phenomena, in: J.M. Delhaye, M. Giot, M.L. Riethmuller (Eds.), Thermohydraulics of two-phase systems for industrial design and nuclear engineering, McGraw-Hill, New York, (1981), pp. 353-403.
24. Yun, G.; Su, G.H.; Wang, J.Q.; Tian, W.X.; Qiu, S.Z.; Jia, D.N.; Zhang, J.W.: Two-phase instability analysis in natural circulation loops of China advanced research reactor, Annals of Nuclear Energy **32** (2005), pp. 379–397.
25. Manera, A.; van der Hagen, T.H.J.J.: Stability of natural-circulation-cooled boiling water reactors during startup: experimental results, Nuclear Technology **143** (2003), pp. 77-88.
26. Subki, M. H.; Aritomi, M.; Watanabe, N.; Kikura, H.; Iwamura, T.: Transport mechanism of thermohydraulic instability in natural circulation boiling water reactors during startup, Journal of Nuclear Science and Technology **40** (2003), pp. 918-931.
27. Jiang, S.Y.; Zhang, Y.J.; Wu, X.X.; Bo, J.H.; Jia, H.J.: Flow excursion phenomenon and its mechanism in natural circulation, Nuclear Engineering and Design **202** (2000), pp. 17–26.
28. Kyung, I.K.; Lee, S.Y.: Experimental observations on flow characteristics in an open two-phase natural circulation loop. Nuclear Engineering and Design **159** (1994), pp. 163-176.
29. Griffith, P.: Geysering in liquid-filled lines, ASME Paper 62-HT-39 (1962).
30. Hands, B.A.: The flow stability of a liquid-nitrogen thermosyphon with 8 mm bore riser, AIChE Symp. Ser. No. 189 Vol. **75** (1979), pp. 177-184.
31. Aritomi, M.; Chiang, J.H.; Nakahashi, T.; Wataru, M.; Mori, M.: Fundamental study on thermo-hydraulics during start-up in natural circulation boiling water reactors (I), Nuclear Science and Technology **29** (1992), pp. 631-641.
32. Fukuda, K.; Kobori, T.: Two-phase flow instability in parallel channels. Proc. 6th International Heat Transfer Conference (1978), FB-17, pp. 369-374.
33. Lee, J. D.; Pan, C.: Nonlinear analysis for a double-channel two-phase natural circulation loop under low-pressure conditions. Annals of Nuclear Energy **32** (2005), pp. 299–329.
34. Baars, A.; Delgado, A.: Multiple modes of a natural circulation evaporator. Int. J. Heat and Mass Transfer **49** (2006), pp. 2304-2314. (DOI 10.1016/j.ijheatmasstransfer.2005.10.046)
35. Paniagua, J.; Rohatgi, U.S.; Prasad, V.: Modeling of thermal hydraulic instabilities in single heated channel loop during startup transients. Nuclear Engineering and Design **193** (1999), pp. 207-226.
36. Jiang, S.Y.; Yao, M.S.; Bo, J.H.; Wu, S.R.: Experimental simulation study on start-up of the 5 MW nuclear heating reactor, Nuclear Engineering and Design **158** (1995), 111-123.
37. Baars, A.: Stationäre und instationäre Betriebszustände eines Naturumlaufverdampfers. Dissertation, Technische Universität München, 2002.

Received 28 March, 2007, accepted 18 May, 2007

Appendix

Table 1 Parameter settings

Heating steam pressure	p_{HS}	0.18...0.45 MPa
Initial feeding subcooling	$\Delta\vartheta_{F\,Sub}$	70 K
Liquid charging level	H	0; 25; 50; 75; 100 mm
Pressure drop coefficient in feeding line	ζ_I	0.4
System pressure		ambient pressure
Working fluid		deionised water

Table 2 Non-dimensional values

Variable	with dimension	non-dimensional
Time	t	$\iota = t / T_U$
Time period of geysering / DWO	T	$T^* = T / T_U$
Mass flow in feeding line	$\dot{m}$	$\dot{m}^* = {}_I \dfrac{T_U}{L_H}$
Subcooling of liquid at inlet (I), exit (E) of heat exchanger and in feeding tank (F)	$\Delta\vartheta_{X\,Sui} = \vartheta_B - \vartheta_X$	$N_{X\,Sub} = \dfrac{c_p \Delta\vartheta_{X\,Sub}}{r} \dfrac{\rho_l - \rho_g}{\rho_g}$

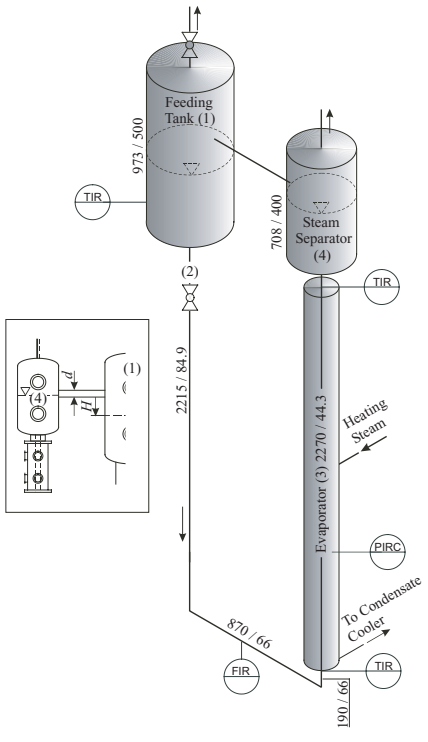

Fig. 1 Steam heated, one tube natural circulation evaporator (Numbers: length tube or tank / inner diameter of tube or tank in mm)

Fig. 2 Depicts the temporal behaviour of mass flow, feeding, inlet, and outlet temperature during start-up of the investigated system for a heating steam pressure of 0.25 MPa and an initial subcooling of around 70 °C.

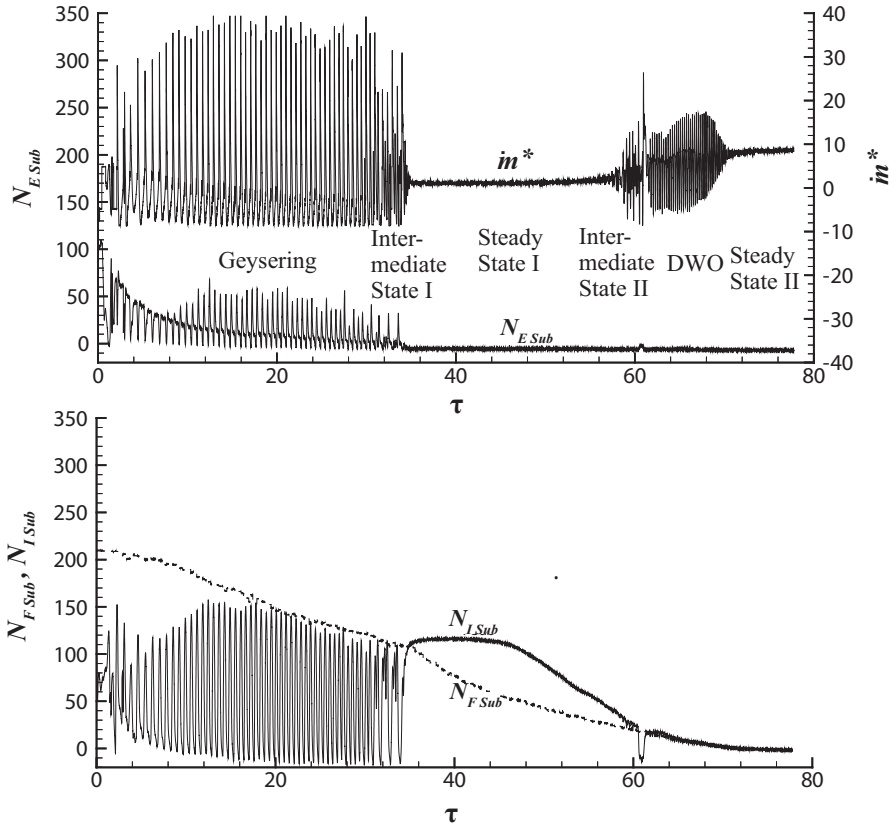

Fig. 2 Mass flow $\dot{m}$, subcooling in feeding line $N_{F\,Sub}$ at the inlet $N_{I\,Sub}$, and exit $N_{E\,Sub}$ of the heated tube versus time τ in dimensionless form for DWO (p = 0.25 MPa, H = 100 mm)

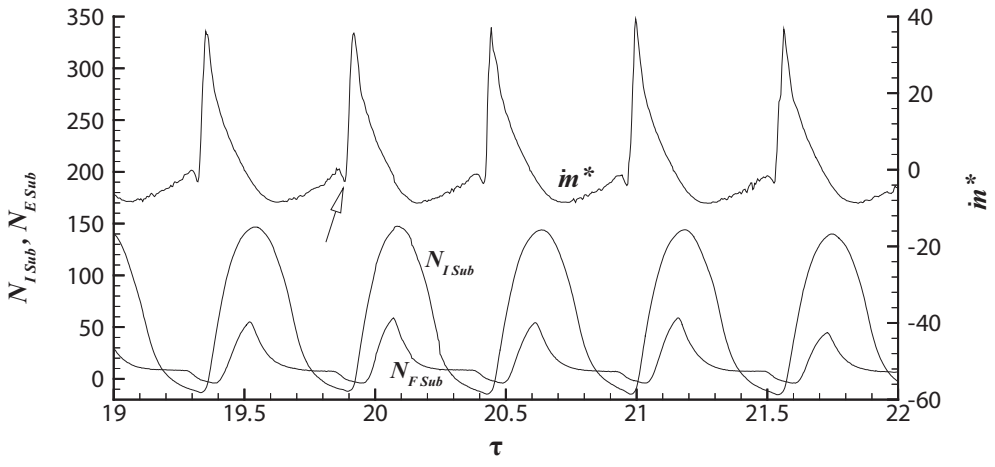

Fig. 3 Mass flow $\dot{m}$, subcooling at the inlet $N_{I\,Sub}$, and exit $N_{E\,Sub}$ of the heated tube versus time τ in dimensionless form for geysering (p = 0.25 MPa, H = 100 mm)

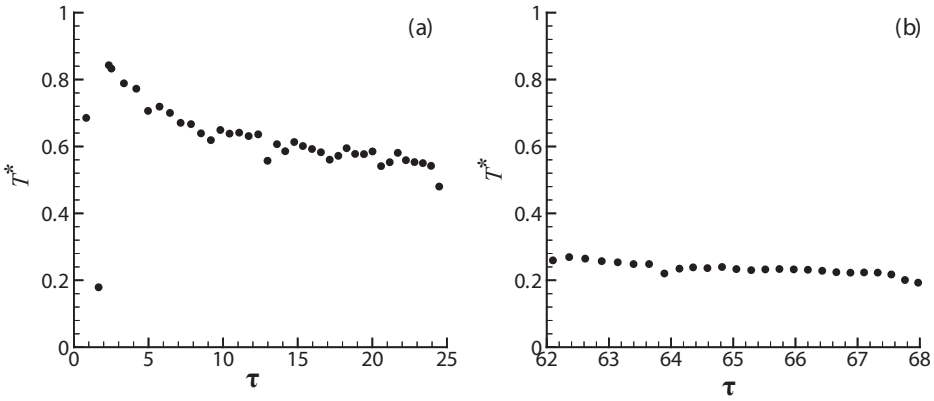

Fig. 4 Development of periodic time during start-up for (a) geysering and (b) density wave oscillations in dimensionless form

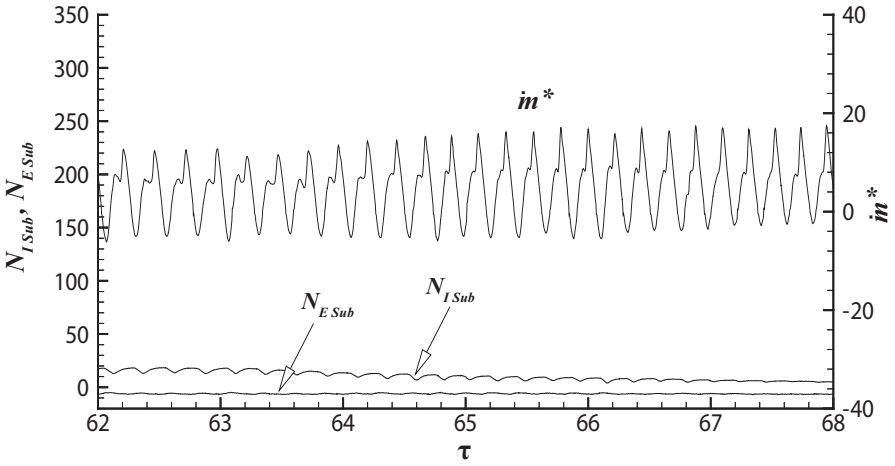

Fig. 5 Mass flow $\dot{m}$, subcooling at the inlet $N_{I\,Sub}$, and exit $N_{E\,Sub}$ of the heated tube versus time τ in dimensionless form for DWO (p = 0.25 MPa, H = 100 mm)

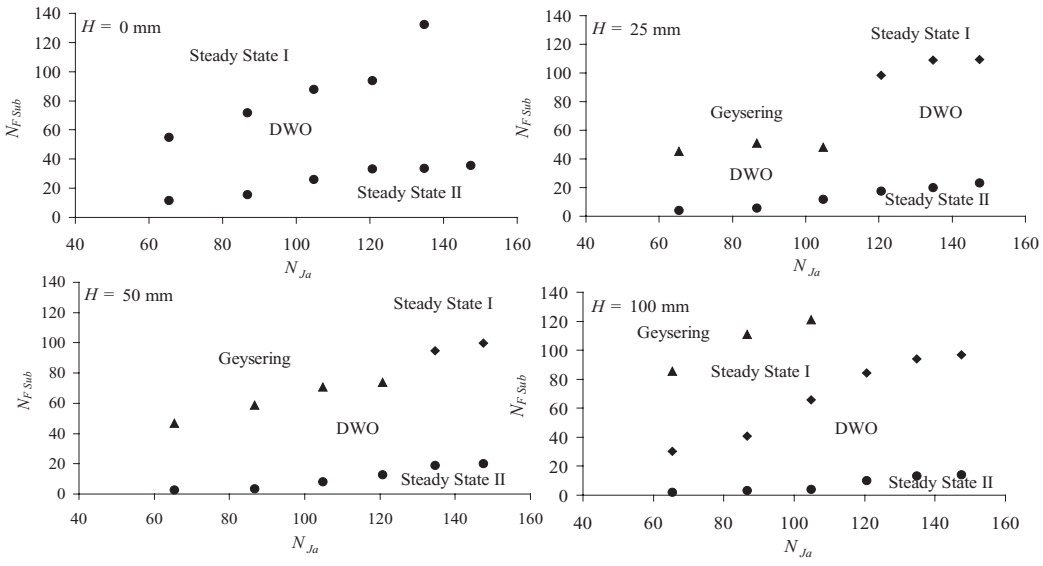

Fig. 6 Stability map with subcooling number $N_{F\,Sub}$ and Jacob number N_{Ja} for different hydrostatic heads H

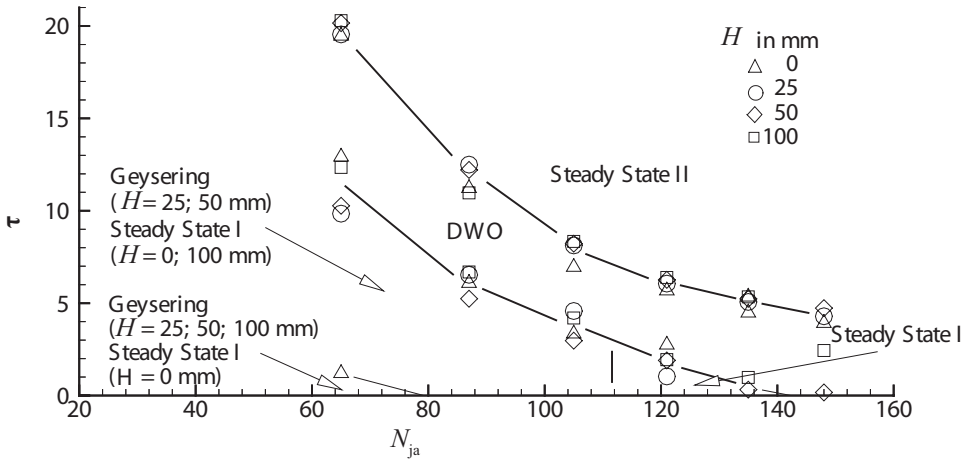

Fig. 7 Time τ to reach the different operational modes versus Jacob number N_{Ja} with parameter hydrostatic head H and initial temperature of 68 °C

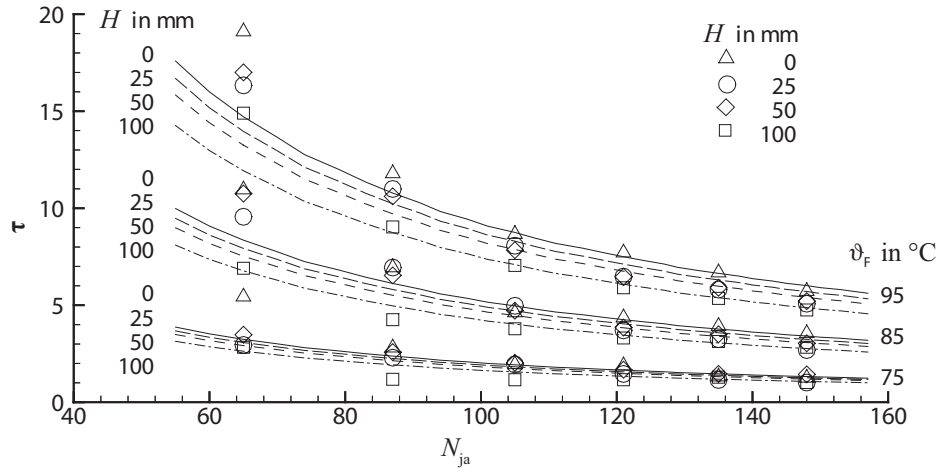

Fig. 8 Heating-up time τ versus Jacob number N_{Ja} with parameter hydrostatic head H and initial temperature of 68 °C, graphs from Eq. (4)